

NONCONFORMING IN TIME DOMAIN DECOMPOSITION METHOD FOR POROUS MEDIA APPLICATIONS

L. Halpern^{*}, C. Japhet[†] and P. Omnes^{‡*}

^{*}LAGA, Université Paris XIII,
99 Avenue J-B Clément, 93430 Villetaneuse, France
e-mail: halpern@math.univ-paris13.fr

[†]CSCAMM, University of Maryland and LAGA, Université Paris XIII,
College Park, MD 20742 USA, 99 Avenue J-B Clément, 93430 Villetaneuse, France
e-mail: japhet@cscamm.umd.edu, japhet@math.univ-paris13.fr

[‡]CEA, DEN, DM2S-SFME-LSET,
F91191 Gif sur Yvette Cedex, France. e-mail: pascal.omnes@cea.fr

Key words: Coupling heterogeneous problems, Optimized Schwarz waveform relaxation, Time discontinuous Galerkin, Different time steps in different layers, Porous media flow

Abstract. *We design a Schwarz waveform relaxation algorithm for solving advection-diffusion-reaction problems in heterogeneous media. The non-overlapping domain decomposition method is global in time and thus allows the use of different time steps in different subdomains. We use a discontinuous Galerkin method in time as a subdomain solver in order to have optimal error estimates and local time stepping. Time windows are used in order to reduce the number of iterations of the algorithm. For applications with widely differing lengths and heterogeneous coefficients, we determine optimal non-local, and optimized Robin transmission conditions, taking into account the size of the domains of small scale. This permits to compute an accurate solution with few iterations in each time window. Numerical results in 2D illustrate the method on an example inspired from nuclear waste disposal simulations.*

1 INTRODUCTION

In the field of nuclear waste management, long term storage within a deep geological formation is one possible strategy. The French Agency for Nuclear Waste Management (ANDRA) is currently carrying out feasibility studies for building such a repository. Far field physical experiments over several hundreds of thousands of years are at best difficult, and one must resort to numerical simulations to evaluate the safety of a proposed disposal.

Far field simulations of underground nuclear waste disposal involve a number of challenges for numerical simulations: widely differing lengths and time-scales, highly variable coefficients and stringent accuracy requirements. In the site under consideration by Andra, the repository would be located in a highly impermeable geological layer, whereas the layers just above and below have very different physical properties. In the clay layer, the radionuclides move essentially because of diffusion, whereas in the dogger layer that is above the main phenomenon is advection³. It is then natural to use time windows for long time computations, with different time steps in the various layers in each time window, so as to match the time step with the physics. To do this, we propose to adapt a global in time domain decomposition method, based on Schwarz waveform relaxation algorithms, to problems in heterogeneous media. This method has been introduced and analyzed for linear advection-reaction-diffusion problems with constant coefficients^{13,8,1} and extended to discontinuous coefficients^{6,2,8,9}, with asymptotically optimized Robin transmission conditions⁶, and semi-discretization in time in one dimension with discontinuous Galerkin^{2,9,12,15}. The method is extended to the bidimensional case in^{9,10}, with convergence results and error estimates for rectangular or strip subdomains.

We extend the method to problems with discontinuous porosity, and domains with highly variable lengths.

Our model problem for the radionuclide transport is the advection-diffusion-reaction equation in $\Omega = \mathbb{R}^2$

$$\varphi \partial_t u + \nabla \cdot (\mathbf{b}u - \nu \nabla u) + cu = f, \quad \text{in } \Omega \times (0, T), \quad (1)$$

with initial condition

$$u(0, x) = u_0(x), \quad x \in \Omega. \quad (2)$$

The advection and diffusion coefficients $\mathbf{b} = (a, b)$ and ν , as well as the reaction coefficient c and the porosity φ , are piecewise smooth, and we suppose $\nu \geq \nu_0 > 0$ *a.e.* in \mathbb{R}^2 . We suppose that $\nabla \cdot \mathbf{b} = 0$. If $\mathbf{b} \in (W^{1,\infty}(\Omega))^2$, $\nu \in W^{1,\infty}(\Omega)$, $c \in L^\infty(\Omega)$, $\varphi \in L^\infty(\Omega)$, if u_0 is in $H^1(\Omega)$, and the right-hand-side f is in $L^2(0, T; L^2(\Omega))$, then there exists a unique weak solution u of (1), (2) in $H^1(0, T; L^2(\Omega)) \cap L^\infty(0, T; H^1(\Omega)) \cap L^2(0, T; H^2(\Omega))$.

2 DOMAIN DECOMPOSITION ALGORITHM

We consider a decomposition of Ω into nonoverlapping subdomains $\Omega_i, i \in \{1, m\}$, with possible corners in the case of Robin transmission conditions. In the case of more general

(second order) transmission conditions, we consider a decomposition in bands. In both cases the boundaries between the subdomains are supposed to be hyperplanes at infinity.

Problem (1) is equivalent to solving m problems in subdomains Ω_i , with coupling conditions on the interface $\Gamma_{i,j}$ between two neighboring subdomains Ω_i and Ω_j given by

$$u_i = u_j, \quad \left(\nu_i \frac{\partial}{\partial \mathbf{n}_i} - \mathbf{b}_i \cdot \mathbf{n}_i\right) u_i = \left(\nu_j \frac{\partial}{\partial \mathbf{n}_i} - \mathbf{b}_j \cdot \mathbf{n}_i\right) u_j \text{ on } \Gamma_{i,j} \times (0, T). \quad (3)$$

Here \mathbf{n}_i is the unit exterior normal to Ω_i and u_i is the restriction of u to Ω_i . To any $i \in \{1, m\}$, we associate the set \mathcal{N}_i of indices of the neighbors of Ω_i . Since the coefficients ν , \mathbf{b} and φ are possibly discontinuous on the interface, we note, for $s \in \Gamma_{i,j}$, $\nu_i(s) = \lim_{\varepsilon \rightarrow 0} \nu(s - \varepsilon \mathbf{n}_i)$. The same notation holds for \mathbf{b} and φ . A simple algorithm based on relaxation of the coupling conditions (3) does not converge in general, not even in the most simple cases¹⁴. Following previous works^{1,6,2,9,10} we propose as preconditioner for the full problem, the sequence of coupled problems :

$$\begin{aligned} \varphi_i \partial_t u_i + \nabla \cdot (\mathbf{b}_i u_i - \nu_i \nabla u_i) + c_i u_i &= f \text{ in } \Omega_i \times (0, T) \\ \left(\nu_i \frac{\partial}{\partial \mathbf{n}_i} - \mathbf{b}_i \cdot \mathbf{n}_i\right) u_i + \mathcal{S}_{i,j} u_i &= \\ \left(\nu_j \frac{\partial}{\partial \mathbf{n}_i} - \mathbf{b}_j \cdot \mathbf{n}_i\right) u_j + \mathcal{S}_{i,j} u_j &\text{ on } \Gamma_{i,j} \times (0, T), j \in \mathcal{N}_i. \end{aligned} \quad (4)$$

where $\mathcal{S}_{i,j}$ are linear operators in time and space, defined by

$$\mathcal{S}_{i,j} \psi = p_{i,j} \psi + q_{i,j} (\partial_t \psi + \nabla_{\Gamma_{i,j}} \cdot (\Pi_{\Gamma_{i,j}} \mathbf{b}_j \psi - \nu_j \nabla_{\Gamma_{i,j}} \psi)), \quad (5)$$

with respectively ∇_{Γ} and $\nabla_{\Gamma} \cdot$ the gradient and divergence operators on Γ , and $\Pi_{\Gamma_{i,j}}$ the tangential trace on $\Gamma_{i,j}$. $p_{i,j}$ and $q_{i,j}$ are functions in $L^\infty(\Gamma_{i,j})$. The case $q_{i,j} = 0$ corresponds to Robin transmission conditions, while $q_{i,j} \neq 0$ corresponds to second order transmission conditions. Under regularity assumptions, solving (1) is equivalent to solving (4) for $i \in \{1, m\}$ with u_i the restriction of u to Ω_i . We now introduce the Schwarz waveform relaxation algorithm for the resolution of (4). An initial guess $(g_{i,j})$ is given on $L^2((0, T) \times \Gamma_{i,j})$ for $i \in \{1, m\}, j \in \mathcal{N}_i$. We solve in each subdomain

$$\varphi \partial_t u_i^k + \nabla \cdot (\mathbf{b}_i u_i^k - \nu_i \nabla u_i^k) + c_i u_i^k = f \text{ in } \Omega_i \times (0, T), \quad (6a)$$

$$\left(\nu_i \frac{\partial}{\partial \mathbf{n}_i} - \mathbf{b}_i \cdot \mathbf{n}_i\right) u_i^k + \mathcal{S}_{i,j} u_i^k = \left(\nu_j \frac{\partial}{\partial \mathbf{n}_i} - \mathbf{b}_j \cdot \mathbf{n}_i\right) u_j^{k-1} + \mathcal{S}_{i,j} u_j^{k-1} \text{ on } \Gamma_{i,j}, j \in \mathcal{N}_i \quad (6b)$$

with initial value (2). The well-posedness and convergence have been analyzed for constant porosity and general decomposition¹⁰. The transmission conditions in (6) imply the coupling conditions (3) at convergence, and lead at the same time to an efficient algorithm, for suitable parameters $p_{i,j}$ and $q_{i,j}$ obtained from an optimization of the convergence factor. Similarly, $\mathcal{S}_{i,j}$ are approximations of the best operators related to

transparent boundary operators ^{4,5}. They can be found using Fourier analysis in the two half-spaces case. This analysis has been done in one dimension with asymptotically optimized Robin transmission conditions for discontinuous coefficients ⁶, and in higher dimension and continuous coefficients ¹. We extend this approach to the bidimensional case and discontinuous coefficients.

2.1 Transmission conditions : two half-spaces analysis

For the analysis of the convergence factor, we suppose that the advection and diffusion coefficients $\mathbf{b} = (a, b)$ and ν , as well as the reaction coefficient c and the porosity φ , are piecewise constant, i.e. constant in each subdomain $\Omega_i, i \in \{1, m\}$. We determine the convergence factor of the algorithm in the two half-spaces case : we split the domain Ω into two subdomains $\Omega_1 = (-\infty, 0) \times \mathbb{R}$ and $\Omega_2 = (0, \infty) \times \mathbb{R}$. Let $e_i^k = u_i^k - u$ be the error in Ω_i at iteration k . The operators $S_{i,j}$ are related to their symbols $\sigma_{i,j}(\eta, \omega)$ by

$$\mathcal{S}_{i,j}u(y, t) = \frac{1}{2\pi} \int \sigma_{i,j}(\eta, \omega) \hat{u}(\eta, \omega) e^{i(\eta y + \omega t)} d\eta d\omega.$$

Using a Fourier transform in time with parameter ω and in y with parameter η , the Fourier transforms \hat{e}_i^k in time and y of e_i^k are solutions of the ordinary differential equation in the x variable

$$-\nu \frac{\partial^2 \hat{e}}{\partial x^2} + a \frac{\partial \hat{e}}{\partial x} + (i(\varphi\omega + b\eta) + \nu\eta^2 + c)\hat{e} = 0. \quad (7)$$

The characteristic roots are

$$r^+(a, \nu, \varphi, \eta, \omega) = \frac{a + \sqrt{d}}{2\nu}, \quad r^-(a, \nu, \varphi, \eta, \omega) = \frac{a - \sqrt{d}}{2\nu}, \quad d = a^2 + 4\nu(i(\varphi\omega + b\eta) + \nu\eta^2 + c).$$

Since $\Re r^+ > 0$, $\Re r^- < 0$, and since we look for solutions which do not increase exponentially in x , we obtain

$$\hat{e}_1^k(x, \eta, \omega) = \alpha_1^k(\eta, \omega) e^{r^+(a_1, \nu_1, \varphi_1, \eta, \omega)x}, \quad \hat{e}_2^k(x, \eta, \omega) = \alpha_2^k(\eta, \omega) e^{r^-(a_2, \nu_2, \varphi_2, \eta, \omega)x}. \quad (8)$$

Inserting (8) into the transmission conditions (6b), we obtain for $k \geq 2$,

$$\alpha_j^{k+1} = \rho \alpha_j^{k-1}, \quad j = 1, 2,$$

with the convergence factor

$$\rho = \frac{a_1 - \nu_1 r^+(a_1, \nu_1, \varphi_1, \eta, \omega) + \sigma_{2,1}}{a_2 - \nu_2 r^-(a_2, \nu_2, \varphi_2, \eta, \omega) + \sigma_{2,1}} \cdot \frac{a_2 - \nu_2 r^-(a_2, \nu_2, \varphi_2, \eta, \omega) - \sigma_{1,2}}{a_1 - \nu_1 r^+(a_1, \nu_1, \varphi_1, \eta, \omega) - \sigma_{1,2}}, \quad \forall \eta, \omega, \text{ in } \mathbb{R}. \quad (9)$$

Hence, the choice for the symbols $\sigma_{i,j}$

$$\sigma_{1,2} = a_2 - \nu_2 r^-(a_2, \nu_2, \varphi_2, \eta, \omega), \quad \sigma_{2,1} = -a_1 + \nu_1 r^+(a_1, \nu_1, \varphi_1, \eta, \omega), \quad (10)$$

leads to convergence in two iterations, independently of the initial guess. This result is optimal since the restriction of the global solution to one subdomain depends on the right-hand side function f on the other subdomain, and thus at least one transmission over the interface is necessary for convergence. However, the corresponding operators are non-local in time and space because of the square-root in $r^\pm(a, \nu, \varphi, \eta, \omega)$, and thus more difficult to implement and costly to use than local ones. We therefore approximate the optimal operators by differential operators, i.e. we approximate the optimal choice $\sigma_{i,j}$ in (10) by polynomials in (η, ω) . We approximate the square roots in the roots of (7) by $p_{i,j} + q_{i,j}(\varphi_j i\omega + b_j i\eta + \nu_j \eta^2)$, which leads to

$$\sigma_{1,2}^{\text{app}} = \frac{p_{1,2} + a_2}{2} + \frac{q_{1,2}}{2}(i\omega + b_2 i\eta + \nu_2 \eta^2), \quad \sigma_{2,1}^{\text{app}} = \frac{p_{2,1} - a_1}{2} + \frac{q_{2,1}}{2}(i\omega + b_1 i\eta + \nu_1 \eta^2), \quad (11)$$

and to the differential operators (5). In order to have effective transmission conditions for low and high frequencies, the parameters $p_{i,j}$ and $q_{i,j}$ are chosen in order to minimize the convergence factor. For Robin transmission conditions, we take $p_{1,2} = p_{2,1} = p$ and we solve the min-max problem

$$\min_p \left(\max_{|\eta| \leq \eta_{\max}, |\omega| \leq \omega_{\max}} \rho(\eta, \omega, p, a_1, a_2, b_1, b_2, \varphi_1, \varphi_2, \nu_1, \nu_2) \right). \quad (12)$$

For Robin 2-sided transmission conditions, we solve the min-max problem

$$\min_{p_{1,2}, p_{2,1}} \left(\max_{|\eta| \leq \eta_{\max}, |\omega| \leq \omega_{\max}} \rho(\eta, \omega, p_{1,2}, p_{2,1}, a_1, a_2, b_1, b_2, \varphi_1, \varphi_2, \nu_1, \nu_2) \right), \quad (13)$$

and for second order transmission condition, the problem

$$\min_{p_{1,2}, q_{1,2}, p_{2,1}, q_{2,1}} \left(\max_{|\eta| \leq \eta_{\max}, |\omega| \leq \omega_{\max}} \rho(\eta, \omega, p_{1,2}, q_{1,2}, p_{2,1}, q_{2,1}, a_1, a_2, b_1, b_2, \varphi_1, \varphi_2, \nu_1, \nu_2) \right), \quad (14)$$

where ρ is given in (9), replacing $\sigma_{i,j}$ by $\sigma_{i,j}^{\text{app}}$. In numerical computations, the frequencies can not be arbitrarily high, but can be restricted to $\omega_{\max} = \frac{\pi}{\Delta t}$, where Δt is the time step, and $\eta_{\max} = \frac{\pi}{\Delta y}$, where Δy is the mesh size over the interface. The min-max problem has been analysed in one dimension⁶. Asymptotical Robin parameters are derived in the case $p_{1,2} = p_{2,1}$ and $\nu_1 \neq \nu_2$, and in the case $p_{1,2} \neq p_{2,1}$ and $\nu_1 = \nu_2$. The most interesting case $p_{1,2} \neq p_{2,1}$ and $\nu_1 \neq \nu_2$ as well as the second order case are currently under investigation.

In the field of nuclear waste computations, domains of meter scale are embedded in domains of kilometer scale. The previous optimization of the convergence factor does not take into account the high variability of the domains lengths. We propose a new approach that takes into account this variability.

2.2 Transmission conditions : three domains analysis

We split the domain $\Omega = \mathbb{R}^2$ into three subdomains $\Omega_1 = (-\infty, 0) \times \mathbb{R}$, $\Omega_2 = (0, L) \times \mathbb{R}$ and $\Omega_3 = (L, \infty) \times \mathbb{R}$ with $L > 0$. Following the same steps as in section 2.1, the solutions of (7) are

$$\begin{aligned} \hat{e}_1^k(x, \eta, \omega) &= \alpha_1^k(\eta, \omega) e^{r^+(a_1, \nu_1, \varphi_1, \eta, \omega)x}, & \hat{e}_3^k(x, \eta, \omega) &= \alpha_3^k(\eta, \omega) e^{r^-(a_3, \nu_3, \varphi_3, \eta, \omega)x}, \\ \hat{e}_2^k(x, \eta, \omega) &= \alpha_2^k(\eta, \omega) e^{r^+(a_2, \nu_2, \varphi_2, \eta, \omega)x} + \beta_2^k(\eta, \omega) e^{r^-(a_2, \nu_2, \varphi_2, \eta, \omega)x} \end{aligned} \quad (15)$$

We set $\xi^k = (\alpha_1^k, \alpha_2^k, \beta_2^k, \alpha_3^k)^t$, and $r_i^\pm = r^\pm(a_i, \nu_i, \varphi_i, \eta, \omega)$. We define

$$D = \frac{a_2 - \nu_2 r_2^+ + \sigma_{2,1}}{a_2 - \nu_2 r_2^- + \sigma_{2,1}} \cdot \frac{a_2 - \nu_2 r_2^- - \sigma_{2,3}}{a_2 - \nu_2 r_2^+ - \sigma_{2,3}} e^{(r_2^- - r_2^+)L} - 1. \quad (16)$$

Remark 2.1 We consider the case $a_i = b_i = 0$. We replace in (16) $\sigma_{i,j}$ by its approximation $\sigma_{i,j}^{app}$ defined in (19)-(20) with $p_{i,j} > 0$ and $q_{i,j} = 0$ (i.e. we consider the Robin approximations). Then D reduces to

$$D = \frac{-\sqrt{d_2} + p_{2,1}}{\sqrt{d_2} + p_{2,1}} \cdot \frac{-\sqrt{d_2} + p_{2,3}}{\sqrt{d_2} + p_{2,3}} e^{-\frac{\sqrt{d_2}}{\nu_2} L} - 1, \quad \text{with } d_2 = 4\nu_2(i\varphi_2\omega + \nu_2\eta^2 + c_2).$$

In that case we have $|D + 1| < 1$ and thus $D \neq 0$. For the general case we suppose that $D \neq 0$.

We insert (15) into the transmission conditions (6b), and obtain for $k \geq 2$,

$$\xi^k = M \xi^{k-1}$$

where the matrix M is defined by

$$M = \begin{pmatrix} 0 & m_{1,2} & m_{1,3} & 0 \\ m_{2,1} & 0 & 0 & m_{2,4} \\ m_{3,1} & 0 & 0 & m_{3,4} \\ 0 & m_{4,2} & m_{4,3} & 0 \end{pmatrix},$$

with

$$\left\{ \begin{aligned} m_{1,2} &= \frac{a_2 - \nu_2 r_2^+ - \sigma_{1,2}}{a_1 - \nu_1 r_1^+ - \sigma_{1,2}}, & m_{1,3} &= \frac{a_2 - \nu_2 r_2^- - \sigma_{1,2}}{a_1 - \nu_1 r_1^+ - \sigma_{1,2}} \\ m_{2,1} &= \frac{a_1 - \nu_1 r_1^+ + \sigma_{2,1}}{a_2 - \nu_2 r_2^- + \sigma_{2,1}} \cdot \frac{a_2 - \nu_2 r_2^- - \sigma_{2,3}}{a_2 - \nu_2 r_2^+ - \sigma_{2,3}} \cdot \frac{e^{(r_2^- - r_2^+)L}}{D}, & m_{2,4} &= -\frac{a_3 - \nu_3 r_3^- - \sigma_{2,3}}{a_2 - \nu_2 r_2^+ - \sigma_{2,3}} \cdot \frac{e^{(r_3^- - r_2^+)L}}{D} \\ m_{3,1} &= -\frac{1}{D} \cdot \frac{a_1 - \nu_1 r_1^+ - \sigma_{2,1}}{a_2 - \nu_2 r_2^- - \sigma_{2,1}}, & m_{3,4} &= \frac{a_2 - \nu_2 r_2^+ + \sigma_{2,1}}{a_2 - \nu_2 r_2^- + \sigma_{2,1}} \cdot \frac{a_3 - \nu_3 r_3^- - \sigma_{2,3}}{a_2 - \nu_2 r_2^+ - \sigma_{2,3}} \cdot \frac{e^{(r_3^- - r_2^+)L}}{D} \\ m_{4,2} &= \frac{a_2 - \nu_2 r_2^+ + \sigma_{3,2}}{a_3 - \nu_3 r_3^- + \sigma_{3,2}} e^{(r_2^+ - r_3^-)L}, & m_{4,3} &= \frac{a_2 - \nu_2 r_2^- + \sigma_{3,2}}{a_3 - \nu_3 r_3^- + \sigma_{3,2}} e^{(r_2^- - r_3^-)L} \end{aligned} \right. \quad (17)$$

Hence, the choice for the symbols $\sigma_{i,j}$

$$\sigma_{1,2} = a_2 - \nu_2 r_2^-, \quad \sigma_{2,1} = -a_1 + \nu_1 r_1^+, \quad \sigma_{2,3} = a_3 - \nu_3 r_3^-, \quad \sigma_{3,2} = -a_2 + \nu_2 r_2^+, \quad (18)$$

leads to $\alpha_2^k = 0$ for $k \geq 1$, $\alpha_1^k = \alpha_3^k = 0$ for $k \geq 2$, and $\beta_2^k = 0$ for $k \geq 3$, and thus leads to convergence in three iterations, independently of the initial guess. This result is optimal since the solution in one subdomain depends on the right-hand side function f on the other subdomains, and thus at least two transmissions over the interface are necessary for convergence. As in section 2.1, we approximate the optimal choice $\sigma_{i,j}$ in (18) by polynomials in (η, ω) :

$$\sigma_{1,2}^{\text{app}} = \frac{p_{1,2} + a_2}{2} + \frac{q_{1,2}}{2}(i\omega + b_2 i\eta + \nu_2 \eta^2), \quad \sigma_{2,1}^{\text{app}} = \frac{p_{2,1} - a_1}{2} + \frac{q_{2,1}}{2}(i\omega + b_1 i\eta + \nu_1 \eta^2), \quad (19)$$

$$\sigma_{2,3}^{\text{app}} = \frac{p_{2,3} + a_3}{2} + \frac{q_{2,3}}{2}(i\omega + b_3 i\eta + \nu_3 \eta^2), \quad \sigma_{3,2}^{\text{app}} = \frac{p_{3,2} - a_2}{2} + \frac{q_{3,2}}{2}(i\omega + b_2 i\eta + \nu_2 \eta^2). \quad (20)$$

In order to simplify the min-max problems, we choose $p_{1,2} = p_{3,2} = p_1$, $q_{1,2} = q_{3,2} = q_1$, $p_{2,1} = p_{2,3} = p_2$, and $q_{2,1} = q_{2,3} = q_2$. Then, the parameters p_i and q_i , $i = 1, 2$, are chosen in order to minimize the convergence factor, i.e. we solve for Robin transmission conditions ($p_1 = p_2 = p$) the min-max problem

$$\min_p \left(\max_{|\eta| \leq \eta_{\max}, |\omega| \leq \omega_{\max}} \rho(\eta, \omega, p, a_1, a_2, a_3, b_1, b_2, b_3, \varphi_1, \varphi_2, \varphi_3, \nu_1, \nu_2, \nu_3, L) \right), \quad (21)$$

for Robin 2-sided transmission conditions, the problem

$$\min_{p_1, p_2} \left(\max_{|\eta| \leq \eta_{\max}, |\omega| \leq \omega_{\max}} \rho(\eta, \omega, p_1, p_2, a_1, a_2, a_3, b_1, b_2, b_3, \varphi_1, \varphi_2, \varphi_3, \nu_1, \nu_2, \nu_3, L) \right), \quad (22)$$

and for second order transmission condition, the problem

$$\min_{p_1, q_1, p_2, q_2} \left(\max_{|\eta| \leq \eta_{\max}, |\omega| \leq \omega_{\max}} \rho(\eta, \omega, p_1, q_1, p_2, q_2, a_1, a_2, a_3, b_1, b_2, b_3, \varphi_1, \varphi_2, \varphi_3, \nu_1, \nu_2, \nu_3, L) \right), \quad (23)$$

where ρ is the spectral radius of the matrix M , in which we have replaced $\sigma_{i,j}$ by $\sigma_{i,j}^{\text{app}}$. The parameters η_{\max} and ω_{\max} are defined as in section 2.1.

2.3 Time discretization with different time steps in the subdomains

In order to reduce the number of iterations of the algorithm and to perform long time computations, we decompose the global time interval into windows $(0, T) = \cup_{\ell=0}^N (T_\ell, T_{\ell+1})$. Then we use, in each time window, the DG-OSWR method ¹⁰ based on a discontinuous Galerkin method in time. Let \mathcal{T}_i be the time partition of $(T_\ell, T_{\ell+1})$ in subdomain Ω_i , with $N_i + 1$ intervals I_n^i , and time step k_n^i . We define interpolation operators \mathcal{I}^i and projection operators \mathcal{P}^i in each subdomain as in ¹⁰. Let $r \geq 1$ be an integer, that we take small in order to make very few iterations in each time window. Let $U_{i,\ell}$ be a discrete approximation of u_i in Ω_i in the window $(T_\ell, T_{\ell+1})$ at step k of the method. $U_{i,\ell}$ is a polynomial of degree at most d on each subinterval I_n^i . Then, the next time window's solution $U_{i,\ell+1}$ in Ω_i is obtained after r DG-OSWR iterations :

for $k = 0, \dots, r - 1$:

$$\begin{aligned}
 \varphi_i \partial_t (\mathcal{I}^i U_{i,\ell}^k) + \nabla \cdot (\mathbf{b} U_{i,\ell}^k - \nu_i \nabla U_{i,\ell}^k) + c_i U_{i,\ell}^k &= \mathcal{P}^i f \text{ in } \Omega_i \times (T_\ell, T_{\ell+1}), \\
 \left(\nu_i \frac{\partial}{\partial \mathbf{n}_i} - \frac{\mathbf{b}_i \cdot \mathbf{n}_i}{2} \right) U_{i,\ell}^k + S_{i,j} U_{i,\ell}^k &= \\
 \mathcal{P}^i \left(\left(\nu_j \frac{\partial}{\partial \mathbf{n}_i} - \frac{\mathbf{b}_j \cdot \mathbf{n}_i}{2} \right) U_j^{k-1} + \tilde{S}_{i,j} U_j^{k-1} \right) &\text{ on } \Gamma_{i,j} \times (T_\ell, T_{\ell+1}), \\
 U_{i,\ell}^k(\cdot, T_\ell) &= U_{i,\ell-1}(\cdot, T_\ell) \text{ in } \Omega_i,
 \end{aligned} \tag{24}$$

where $S_{i,j} U$ is defined by $S_{i,j} U = p_{i,j} U + q_{i,j} (\varphi_j \partial_t (\mathcal{I}^j U) + \nabla_{\Gamma_{i,j}} \cdot (\Pi_{\Gamma_{i,j}} \mathbf{b}_j U - \nu_j \nabla_{\Gamma_{i,j}} U))$, and $\tilde{S}_{i,j} U = p_{i,j} U + q_{i,j} (\varphi_j \partial_t (\mathcal{I}^j U) + \nabla_{\Gamma_{i,j}} \cdot (\Pi_{\Gamma_{i,j}} \mathbf{b}_j U - \nu_j \nabla_{\Gamma_{i,j}} U))$.

The coefficients $p_{i,j}$ and $q_{i,j}$ are defined through the previous optimization procedure, and such that the subdomain problems be well-posed. They are taken constant along the interface, as the mean value of the parameters obtained by a numerical optimization of the convergence factor. The semi-discrete in time analysis was performed for a constant porosity⁹. We have implemented the algorithm with \mathbf{P}_1 finite elements in space in each subdomain.

3 NUMERICAL RESULTS

We have implemented the algorithm defined in section 2.3 with $d = 1$. We consider an example in two dimensions with a repository inside a host rock (clay) inspired from nuclear waste disposal simulations³.

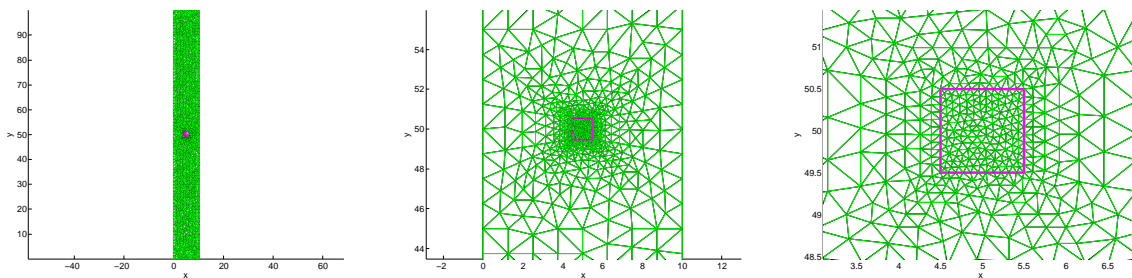


Figure 1: Computational domain, with a zoom from the left to the right. The repository is inside the magenta square

3.1 The test case

The computational domain (in meters) is $\Omega = (0, 10) \times (0, 100)$, and is decomposed into two subdomains: $\Omega_1 = (4.5, 5.5) \times (49.5, 50.5)$ for the repository, and $\Omega_2 = \Omega \setminus \Omega_1$ for the host rock, as shown on Figure 1. The final time is $T = 10^{11}$ s (i.e. approximately 10^4 years). The initial value

is $u_0 = 0$ in the host rock and $u_0 = 1$ in the repository, and the right-handside is $f = 0$. The reaction c is zero, the diffusion and porosity are $\nu_1 = 10^{-11} m^2/s$, $\varphi_1 = 1$ in the repository and $\nu_2 = 6.10^{-13} m^2/s$, $\varphi_2 = 0.06$ in the host rock. The advection field is a Darcy flow, computed with a finite volume method (see Figure 2):

$$\begin{aligned} \operatorname{div}(\mathbf{b}) &= 0 \\ \mathbf{b} &= -K\nabla h \end{aligned}$$

with $K = k \operatorname{Id}$, where Id is the identity matrix, and $k = 10^{-8}$ in the repository and $k = 10^{-13}$ in the clay. For the Darcy flow, we take homogeneous Neumann boundary conditions at $x = 0$ and $x = 10$ and Dirichlet conditions with $h = 100$ at $y = 0$ and $h = 0$ at $y = 100$. For the convection-diffusion equation, we choose homogeneous Neumann boundary conditions at $x = 0$ and $x = 10$ and homogeneous Dirichlet conditions at $y = 0$ and $y = 100$.

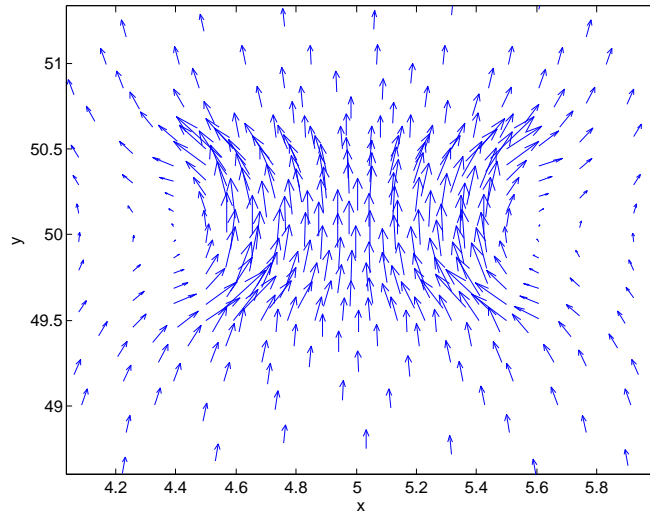


Figure 2: Darcy flow

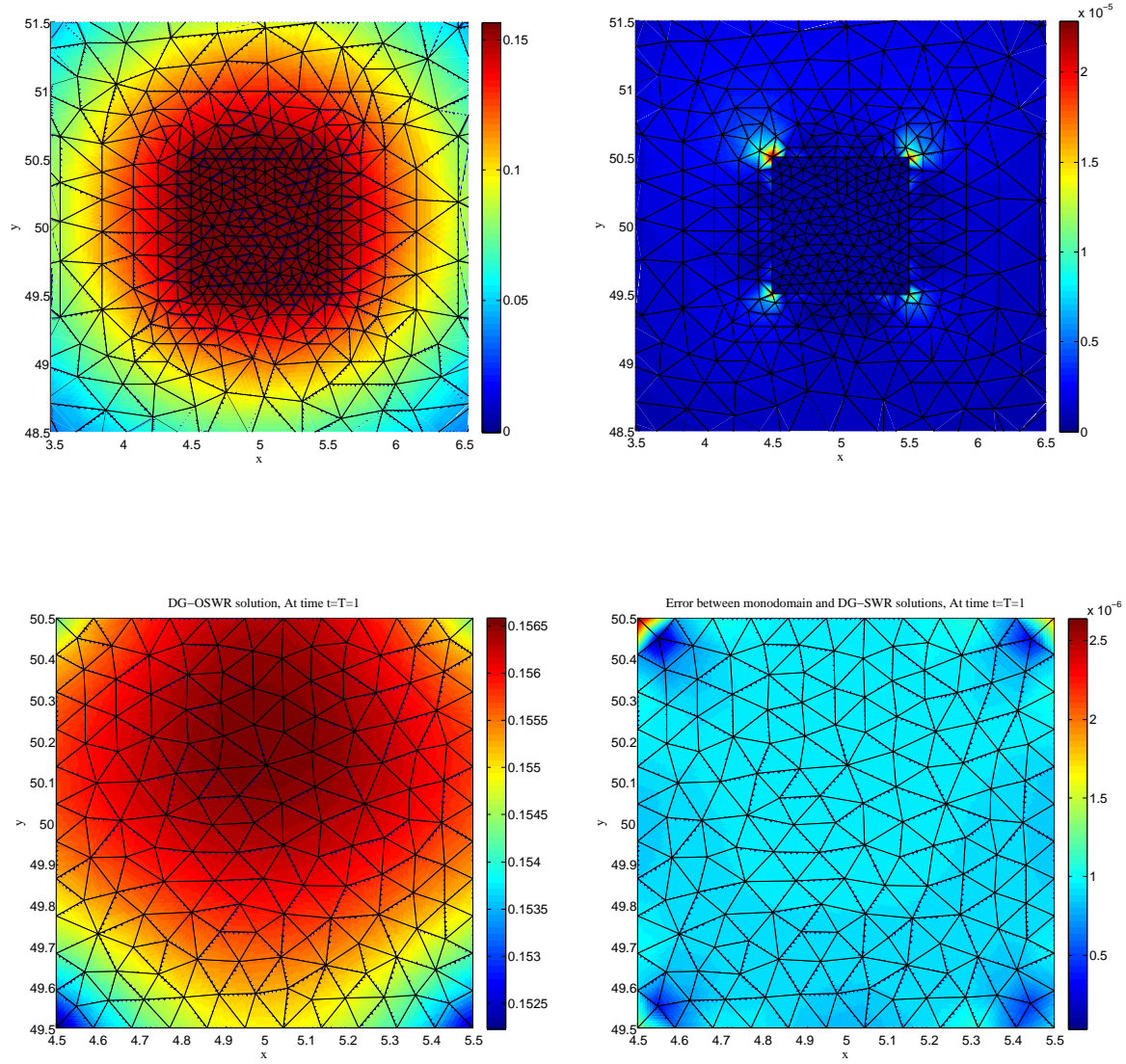


Figure 3: Comparison between variational and nonconforming DG-OSWR solutions at final time $t = 1$. Left top: approximate solution (clay), Left bottom: approximate solution (repository), Right top: error with the variational solution (clay), Right bottom: error with the variational solution (repository)

3.2 An example of DG-OSWR solution with time windows

We first give an example of a multidomain solution with 10 time windows. On Figure 3, we compare the approximate solution computed using 4 iterations to the variational solution computed in one time window on a conforming finer space-time grid with time step $k = 1/500$. We observe at final time $T = 1$ that the approximate solution is close to the variational solution, as we can see on the errors on the right figures (top for the clay, and bottom for the repository).

3.3 Convergence analysis versus the parameters $p_{i,j}$ and $q_{i,j}$

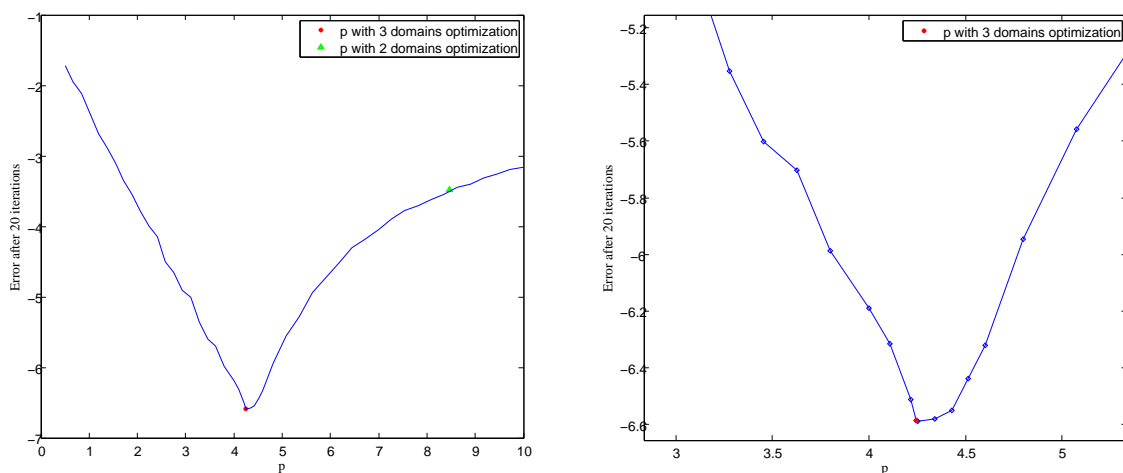


Figure 4: Error after 20 iterations for various values of the parameters p , with a zoom from the left to the right. Left: the lower left star marks the parameter derived from a numerical minimization of the three domains convergence rate, whereas the upper right cross shows the parameter, as found by numerically minimizing the two half-spaces convergence rate. Right: Zoom into left figure near the optimal value.

We first consider the one dimensional problem

$$\varphi \partial_t u + \frac{d}{dx} \left(au - \nu \frac{du}{dx} \right) + cu = f, \quad \text{in } \Omega \times (0, T), \quad (25)$$

with $\Omega = (0, 1)$ and $T = 4/100$. The domain Ω is decomposed into three subdomains: $\Omega_1 = (0, 0.4965)$, $\Omega_2 = (0.4965, 0.5035)$ and $\Omega_3 = (0.5035, 1)$. The domain Ω_2 represents the repository, and Ω_1 and Ω_3 the host rock. The initial value is $u_0 = 0$ in the host rock and $u_0 = 1$ in the repository, and the right-hand side is $f = 0$. The reaction c is zero, the diffusion and porosity

are $\nu_2 = 1$, $\varphi_1 = 1$ for the repository and $\nu_1 = \nu_3 = 0.06$, $\varphi_1 = \varphi_3 = 0.06$ for the host rock. The advection field a is constant equal to 1 in each subdomain. The time steps are $k_2 = T/500$

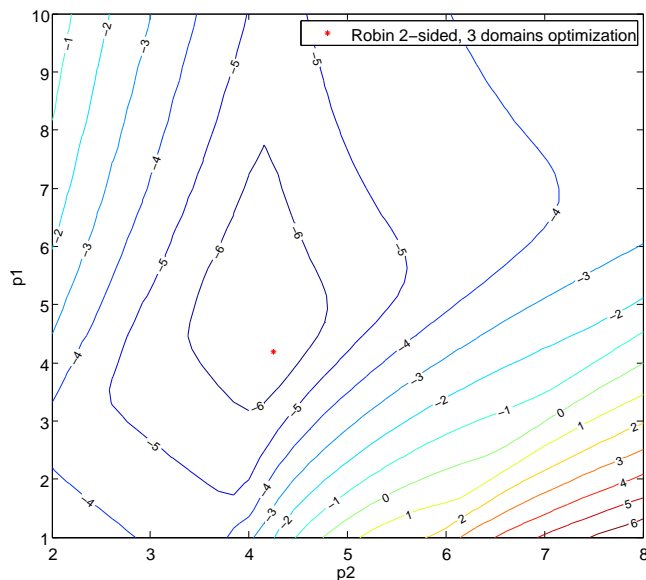


Figure 5: Level curves of the error after 20 iterations, the star marks the parameter derived from a numerical minimization of the three domains convergence rate

in the repository and $k_1 = k_3 = T/100$ in Ω_1 and Ω_3 . The mesh size is $h_2 = 0.007/20$ in the repository and $h_1 = h_3 = 0.4965/200$ in the host rock.

In the one dimensional case, the Order 2 conditions reduce to Order 1 conditions :

$$\mathcal{S}_{i,j}\psi = p_{i,j}\psi + q_{i,j}\partial_t\psi.$$

We consider first the Robin case. We solve numerically problems (12) for the 2 half-spaces optimization, and (21) for the 3 domains optimization. We show on Figure 4 the norm of the error in $L^\infty(0, T, L^2(\Omega_i))$ after 20 iterations when running the algorithm on the discretized problem, for various values of the parameter p , with random initial guess on the interfaces. We observe that the value found by minimizing the three-domains convergence rate (21) is close to the optimal value, compared to the parameter corresponding to the value found by minimizing the two half-spaces convergence rate (12).

On Figure 5 we consider the Robin 2-sided case. We show the level curves of the error after 20 iterations, when running the algorithm on the discretized problem, for various values of the parameters $p_{1,2}$ and $p_{2,1}$ for problem (13), and p_1 and p_2 for problem (22). We observe that the value found by minimizing the three-domains convergence rate (22) is close to the optimal value. The value found by minimizing the two half-spaces convergence rate (13) is around $p_{1,2} = 1.7389$, $p_{2,1} = 70.284$, and the converge is very poor in that case, as we can see on Figure 6.

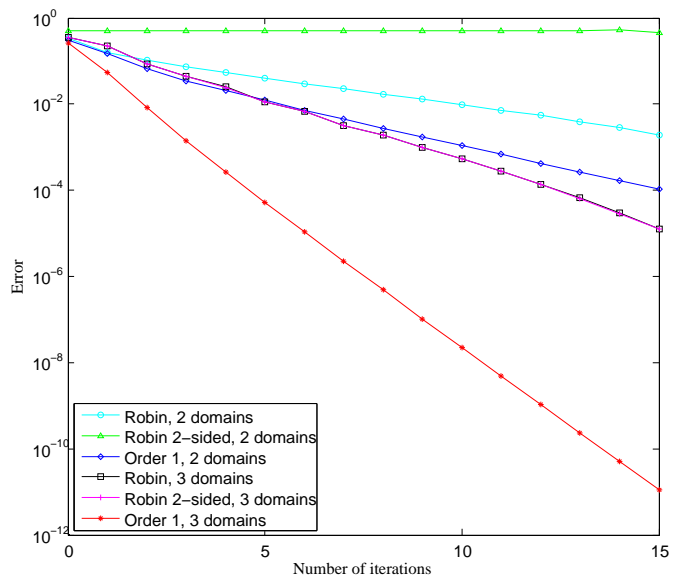


Figure 6: Error curves versus the iterations for various values of the parameters.

On Figure 6 we show the error curves versus the iterations, for the different values of the parameters, when starting with a null initial guess, and initial value $u_0 = 0$ in the host rock and $u_0 = 1$ in the repository. As the time grids are nonconforming in time, a reference solution is computed such that the residual is smaller than 10^{-12} . We observe that the error between the multidomain and the reference solutions decreases much faster with the Order 1 transmissions conditions obtained from a numerical optimization of the three domains convergence factor. We also observe that the Robin parameter, as the Robin 2-sided parameters, obtained from a

numerical optimization of the three domains convergence factor, lead to similar error curves. For both cases the errors decrease faster than with the Order 1 transmissions conditions obtained from a numerical optimization of the two half-spaces convergence factor.

We now consider the bidimensional test case of Section 3.1 with parameters computed numerically (with `fminsearch`) from the minimization problem (23), with $p_1 = p_2 = p$, $q_1 = q_2 = q$ as a first step. On Figure 7 (left) we show the level curves of the error after 20 iterations, when running the algorithm on the discretized problem, for various values of the parameters p and q . The star represents the value found by minimizing the three-domains convergence rate (23) and is close to the optimal value. On the right figure of Figure 7 we show the error curves versus the iterations, for the different values of the parameters, when starting with a null initial guess, and initial value $u_0 = 0$ in the host rock and $u_0 = 1$ in the repository. A reference solution is computed such that the residual is smaller than 10^{-12} . We observe that the error between the multidomain and the reference solutions decreases much faster with the Order 2 transmissions conditions obtained from a numerical optimization of the three domains convergence factor, than with the transmissions conditions obtained from a numerical optimization of the two half-spaces convergence factor.

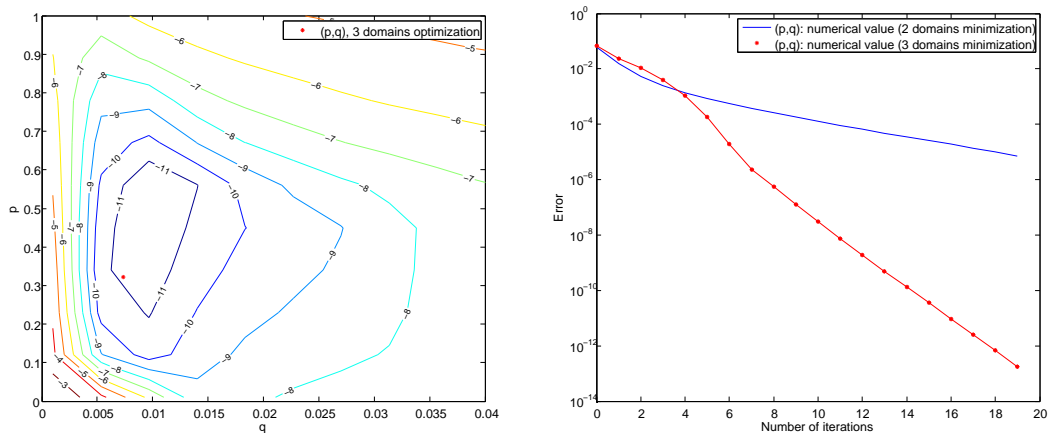


Figure 7: Left: level curves of the error after 20 iterations, the star marks the parameter derived from a numerical minimization of the three domains convergence rate. Right: error curves versus the iterations.

3.4 Convergence analysis versus the time step

We analyze now the precision in time in one time window. The DG-OSWR converged solution is such that the residual is smaller than 10^{-12} . We compute a variational reference solution on

a time grid with 8192 time steps. The nonconforming solutions are interpolated on the previous grid to compute the error. We start with a time grid with 128 time steps for the repository and 28 time steps for the host rock. Thereafter the time steps are divided by 2 several times. The left figure of Figure 8 shows the relative error in norm $L^2(I; L^2(\Omega_i))$ versus the number of refinements, for both subdomains. We have represented also the relative error between the reference solution and a monodomain variational solution. For the fine grid solution we start with 128 time steps, and for the coarse grid solution we start with 28 time steps, and we divide the time steps by 2 several times. We observe that the error obtained in the nonconforming case, in the subdomain where the grid is finer, is nearly the same as the error obtained in the monodomain finer case. On the right figure of Figure 8 we show the relative error in $L^2(\Omega_i)$ at final time $t = T$ versus the time steps, for both subdomains and in the monodomain case. We observe the order 3 in time for the nonconforming case as for the monodomain case¹⁵.

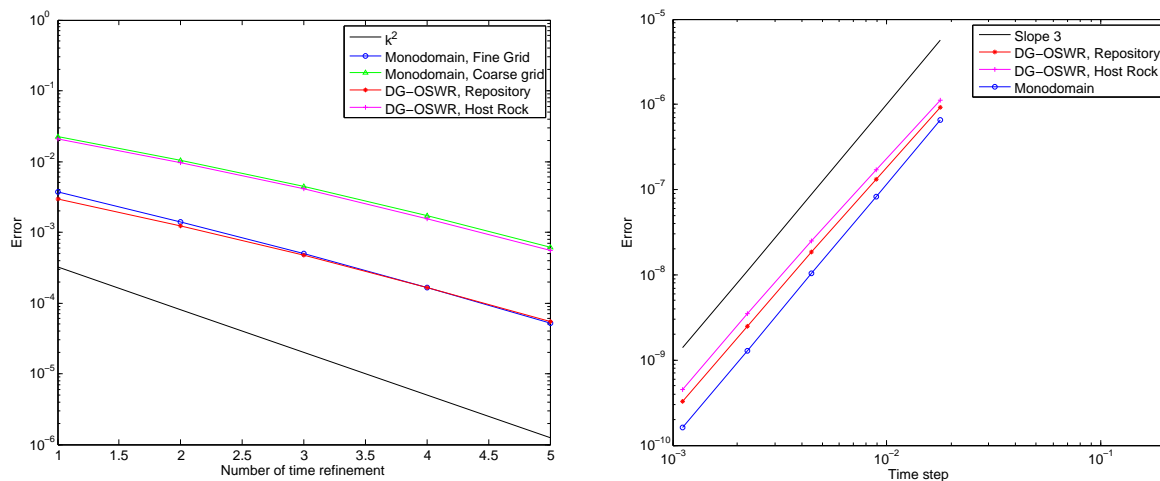


Figure 8: Relative error between variational and DG-OSWR solutions versus the refinement in time. On the left, the norms of the error in $L^2(I; L^2(\Omega_i))$, on the right the L^2 error at final time

4 CONCLUSIONS

We have extended the DG-OSWR method to porous media problems, and we proposed optimized transmission conditions that take into account the high variability of length of the domains. We have shown numerically that taking into account this variability is of importance and can

improve drastically the convergence of the algorithm. The method preserves the order of the monodomain scheme in the case of discontinuous variable coefficients, different time steps in the subdomains and domains of highly differing lengths. An analysis of the influence of the decomposition in time windows and of the computation costs is in progress.

REFERENCES

- [1] D. Bennequin, M.J. Gander and L.Halpern, A homographic best approximation problem with application to optimized Schwarz waveform relaxation, *Math. Comp.*, **Vol. 78**, 185–223 (2009).
- [2] E. Blayo, L. Halpern and C. Japhet, Optimized Schwarz waveform relaxation algorithms with nonconforming time discretization for coupling convection-diffusion problems with discontinuous coefficients, *Decomposition Methods in Science and Engineering XVI, Lecture Notes in Computational Science and Engineering*, O.B. Widlund and D.E. Keyes eds., **Vol. 55**, 267–274, Springer (2007).
- [3] Alain Bourgeat, Michel Kern, Stephan Schumacher and Jean Talandier, The Couplex test cases: Nuclear waste disposal simulation. *Computational Geosciences*, **Vol. 8**, n° 2, 83–98 (2004). Special Issue: Simulation of Transport Around a Nuclear Waste Disposal Site: The Couplex Test Cases (Editors: Alain Bourgeat and Michel Kern).
- [4] P. Charton, F. Nataf, and F. Rogier, Méthode de décomposition de domaine pour l'équation d'advection-diffusion, *C.R. Acad. Sci.* **313**, n° 9, 623–626 (1991).
- [5] M.J. Gander, L. Halpern and F. Nataf, Optimal convergence for overlapping and non-overlapping Schwarz waveform relaxation, *Eleventh international Conference of Domain Decomposition Methods* (C-H Lai, P. Bjorstad, M. Cross, and O. Widlund eds.), ddm.org, (1999)
- [6] M.J. Gander, L. Halpern and M. Kern, Schwarz Waveform Relaxation Method for Advection–Diffusion–Reaction Problems with Discontinuous Coefficients and non-Matching Grids, *Domain Decomposition Methods in Science and Engineering XVI, Lecture Notes in Computational Science and Engineering*, O.B. Widlund and D.E. Keyes eds., **Vol. 55**, 916–920, Springer (2007).
- [7] M.J. Gander and L. Halpern, Optimized Schwarz Waveform Relaxation Methods for Advection Reaction Diffusion Problems, *SIAM Journal on Numerical Analysis*, **Vol. 45**, n° 2, 666–697 (2007).
- [8] L. Halpern and C. Japhet, Discontinuous Galerkin and Nonconforming in Time Optimized Schwarz Waveform Relaxation for Heterogeneous Problems, *Domain Decomposition Methods in Science and Engineering XVII, Lecture Notes in Computational Science and Engineering*, U. Lange, M. Discacciati, D.E. Keyes, O.B. Widlund and W. Zulehner eds., **Vol. 60**, 211–219, Springer (2008).

- [9] L. Halpern, C. Japhet and J. Szeftel, Discontinuous Galerkin and nonconforming in time optimized Schwarz waveform relaxation, *Proceedings of the Eighteenth International Conference on Domain Decomposition Methods*, <http://numerik.mi.fu-berlin.de/DDM/DD18/> in electronic form, to appear in printed form in the proceedings of DD19, (2009).
- [10] L. Halpern, C. Japhet and J. Szeftel, Space-time nonconforming Optimized Schwarz Waveform Relaxation for heterogeneous problems and general geometries, accepted for publication in *Proceedings of the Nineteenth International Conference on Domain Decomposition Methods*.
- [11] C. Johnson, K. Eriksson and V. Thomee, Time discretization of parabolic problems by the discontinuous Galerkin method, *RAIRO Modél. Math. Anal. Numér.*, **Vol. 19**, 611–643 (1985).
- [12] C. Makridakis and R. Nochetto, A posteriori error analysis for higher order dissipative methods for evolution problems, *Numer. Math.*, **Vol. 104**, n° 4, 489–514 (2006)
- [13] V. Martin, An optimized Schwarz waveform relaxation method for the unsteady convection diffusion equation in two dimensions, *Appl. Numer. Math.*, **Vol. 52**, 401–428 (2005).
- [14] Alfio Quarteroni and Alberto Valli, Domain Decomposition Methods for Partial Differential Equations, *Oxford Science Publications* (1999).
- [15] V. Thomee, Galerkin Finite Element Methods for Parabolic Problems, *Springer* (1997).